

# **MASS TRANSPORT IN FLOWING BLOOD: AUGMENTATION OF SOLUTE TRANSPORT NEAR THE WALL OF A CIRCULAR CONDUIT**

Arthur J. Schwartz

Department of Chemical Engineering and Materials Science  
University of Minnesota

*A polarographic technique using flush mounted electrodes in the wall of a tube was used to measure augmentation of diffusion in flowing suspensions of bovine red blood cells in a region close to the tube wall. The effective diffusion coefficient was found to be an increasing function of particle Peclet number (based on the wall shear rate) and volume fraction of cells. Comparison of these results with experimentally measured diffusion augmentation in a system where wall effects were negligible provides information on the behavior of the cell-free skimming layer at the tube wall. The thickness of this skimming layer is dependent on the wall shear rate and on the bulk hematocrit. Below hematocrits of 25% the skimming layer thickness decreases with increasing wall shear rate, while above 25% hematocrit the skimming layer becomes thicker as the wall shear rate increases.*

## **INTRODUCTION**

Diffusion of solutes near surfaces in flowing blood is of great importance in artificial organs such as oxygenators and dialyzers and has been suggested as an important factor in the filtration theory of atherosclerosis (5). In the bulk of flowing blood, particle induced diffusion augmentation greatly increases the effective diffusion coefficient of solutes in the continuous phase. Near the wall of a conduit, however, the presence of a cell-free skimming layer may eliminate this effect and limit the transport rate of solutes moving to and from the wall. Also, regions of separated flow, such as occur at branch points, may show lowered shear rates and thus reduce diffusional augmentation.

By using a diffusion controlled redox reaction taking place on a small electrode mounted flush with the wall of a tube, the effective diffusion

---

Address for correspondence: Arthur J. Schwartz, Miles Laboratories, Inc., P.O. Box 932, Elkhart, Indiana 46515.

The author wishes to acknowledge Professor Kenneth H. Keller of the Department of Chemical Engineering and Materials Science, University of Minnesota, for his contribution as graduate advisor for the author's doctoral research, a portion of which is summarized here.

coefficient of the reacting solute may be measured in a flowing suspension of red blood cells. Since essentially all of the mass transfer of this solute takes place in a thin region (20–30  $\mu$  thick) near the wall, the results are not expected to agree with any of the theoretical models which attempt to describe diffusional augmentation in the bulk of a fluid (2,6,8). Moreover, recent experiments (11,12) indicate that none of these models are satisfactory.

The present study was undertaken to measure augmentation of solute transport near the wall of a tube under conditions of fully developed laminar flow. The augmented diffusion coefficients measured here were larger than those obtained by Wang (11,12) who worked in a system where wall effects were unimportant. This can be explained by postulating the presence of a cell-free skimming layer along the tube wall. By comparing the present results with Wang's (11,12), a quantitative description of this skimming layer can be obtained.

### TECHNIQUE

A polarographic technique which involves the reduction of ferricyanide ion on the surface of a small electrode mounted flush with the wall of a tube has been used previously (7,9) to measure local fluid shear rates at the electrode surface. By modifying the electrolyte composition and electrode material, the technique was used to measure effective diffusion coefficients in a flowing suspension of red blood cells. The measured diffusion coefficients are characteristic of mass transfer in a thin (20–30  $\mu$ ) region adjacent to the tube wall and are influenced by the presence of the wall.

For these experiments a tube six feet long and one-quarter inch in diameter was used. Test electrodes were either pure platinum or a platinum–rhodium alloy and ranged in diameter from 0.013 to 0.036 cm. The electrodes were mounted flush with the tube wall and placed halfway down the length of the tube. They were thus in a region where the fluid velocity profile for a homogeneous fluid would be fully developed. A large reference electrode was placed upstream of the entrance to the tube. The electrolyte-cell suspension was recirculated between two constant head tanks with overflow, and flow through the tube was controlled by throttling the output of the tube.

The electrolyte consisted of an equimolar solution of potassium ferri- and ferrocyanide and the total ionic concentration was adjusted to be isotonic with the red blood cells. The ionic strength of the electrolyte was high enough so that the electric field near each electrode was sufficiently damped to avoid ionic migration. Fresh cattle blood was collected at a local slaughter house in ACD anticoagulant. The red cells were removed by centrifugation and washed several times in isotonic saline before being resuspended in the electrolyte for use in these experiments.

The technique has been thoroughly discussed elsewhere (7,9) so only a brief summary is needed here. When a potential difference is imposed

between the test and reference electrodes, with the test electrode negative, a current will flow due to the reduction of ferricyanide on the test electrode and the oxidation of ferrocyanide on the reference electrode. If this potential difference is large enough, and the sizes of the electrodes appropriate, the current is limited by the diffusion of ferricyanide to the test electrode. For a homogeneous fluid this limiting current is described by the relation

$$i_l = W\pi Fnc_b d^{5/3} D_B^{2/3} \beta^{1/3} , \quad (1)$$

where  $W$  = constant depending on electrode shape = 0.216 for a circular electrode

$F$  = Faraday's constant = 96,500 C/equivalent

$n$  = number of electrons transferred per molecule

$c_b$  = bulk concentration of ferricyanide

$d$  = electrode diameter

$D_B$  = Brownian diffusion coefficient of ferricyanide

$\beta$  = wall shear rate.

When the fluid is a suspension of particles which are impermeable to the species being transported, the limiting current may be used to define an effective diffusion coefficient,  $D_E$ ,

$$i_l = W\pi Fnc_b d^{5/3} D_E^{2/3} \beta^{1/3} (1 - \phi)^{1/3} , \quad (2)$$

where  $\phi$  = volume fraction of particles. The factor  $(1 - \phi)$  appears due to the fact that the solute does not penetrate the particles.

## RESULTS

Data from the experiments are shown in Figs. 1 and 2 and Table 1. The independent variable is the particle Peclet number based on the wall shear rate,  $\beta$ , and on the major diameter of the cell,  $a$ ,

$$Pe = \frac{a^2 \beta}{D_B} . \quad (3)$$

The dependent variable is the augmentation,  $A_x$ , defined as

$$A_x = \frac{D_E}{D_F} - 1 . \quad (4)$$

$D_F$  is the diffusion coefficient predicted by Fricke (3) for a stagnant suspension.  $D_F$  takes into account the distortion of the solute diffusion paths due to the interference of the cells but does not account for any fluid mixing due to motion of the particles. For impermeable prolate ellipsoids

$$D_F = D_B \left[ \frac{1 - \phi}{1 - \phi(1-G)} \right] \quad (5)$$

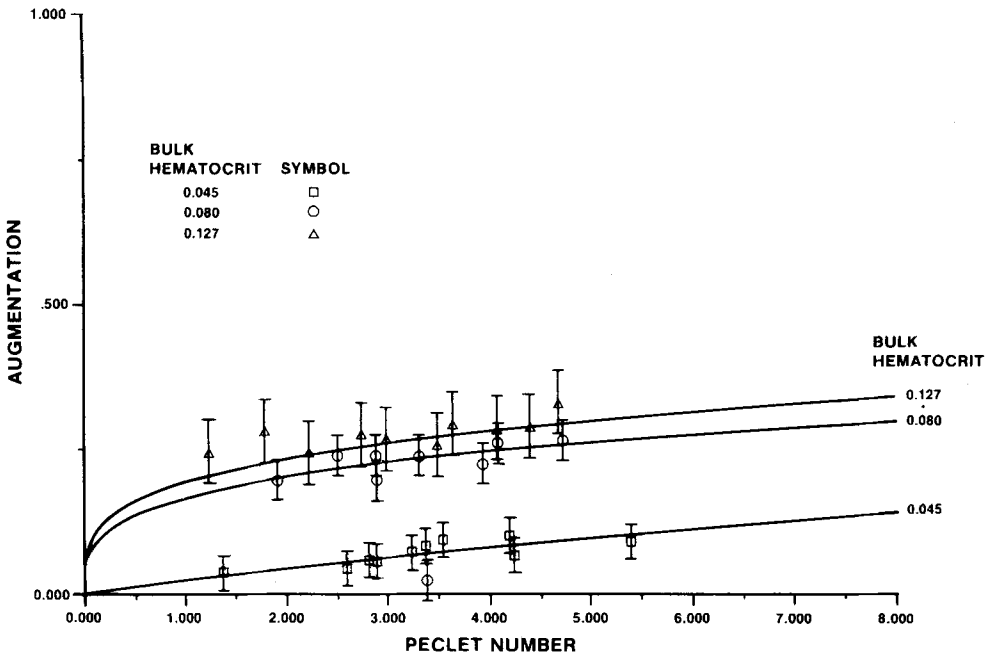


FIGURE 1. Augmentation vs particle Peclet number for  $\phi = 0.045, 0.080, 0.127$ . Vertical bars represent  $\pm 1$  standard deviation.

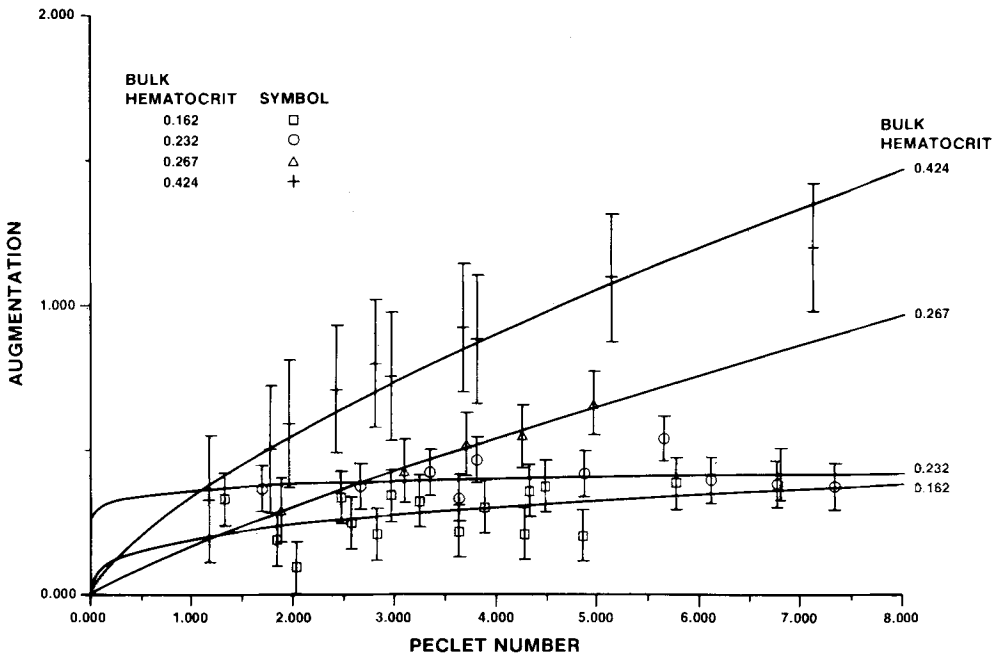


FIGURE 2. Augmentation vs particle Peclet number for  $\phi = 0.162, 0.232, 0.267, 0.424$ . Vertical bars represent  $\pm 1$  standard deviation.



where  $G$  is a shape factor equal to 1.79 for bovine red blood cells. In all cases  $D_E$  for the sheared cell suspensions was larger than  $D_F$ , indicating the presence of augmented diffusion.

### DISCUSSION

The thickness of the region near the wall where the augmented transport is measured,  $\delta_c$ , depends on the electrode size, fluid shear rate and fluid parameters (see Appendix I)

$$\delta_c = 1.687 \left[ \frac{D_F d}{\beta(1-\phi)} \right]^{1/3} \quad (6)$$

Due to random experimental errors, no significant difference in response was detected from electrodes of different sizes. Because of this, the data were averaged over all electrodes at each flow rate and hematocrit and it was not possible to get information on cell distributions directly from the experiments.

Information on the cell distribution can be recovered, however, using the data of Wang (11,12). The results of her experimental measurements of diffusion augmentation in the bulk of a cell suspension can be empirically expressed as

$$A_0 = (a_1 \cdot \phi^2 + a_2 \cdot \phi) \cdot Pe^m \quad (7)$$

with  $a_1 = -1.035$ ,  $a_2 = 0.594$ , and  $m = 0.85$  (10). The lines shown in Figs. 1 and 2 are the empirical curves

$$A_x = a_0 \cdot Pe^b \quad (8)$$

where  $a_0$  and  $b$  depend on  $\phi$  and are chosen by a least squares fit to the data. These values are listed in Table 2.

Except for  $\phi = 0.045$ , the augmentations measured in the present study are higher than those reported by Wang (11,12). This can be explained by postulating a local cell volume fraction,  $\phi_l$ , within the concentration boundary layer that is lower than the bulk cell volume fraction,  $\phi_b$ . The

TABLE 2. Coefficients for Eq. 8

$\phi$	$a_0$	$b$
0.045	0.025	0.832
0.080	0.165	0.288
0.127	0.194	0.270
0.162	0.193	0.327
0.232	0.363	0.074
0.267	0.171	0.834
0.424	0.340	0.704

local hematocrit may be estimated by the procedure described in Appendix II. The results are shown in Fig. 3.

In reality the local cell volume fractions shown in Fig. 3 are averages of the actual cell distribution,  $\phi(y)$ , in the concentration boundary layer

$$\phi_l = \frac{1}{\delta_c} \int_0^{\delta_c} \phi(y) dy \quad (9)$$

where  $y$  is the distance from the wall. One approach to modeling this is to assume the existence of a skimming layer for which  $\phi(y)=0$  (cell-free) for  $y < \delta_s$  and  $\phi(y)=\phi_b$  for  $y \geq \delta_s$ . Then, using Eq. 6

$$\delta_s = 1.687 \left( 1 - \frac{\phi_l}{\phi_b} \right) \left[ \frac{D_{F_l} d}{\beta(1 - \phi_l)} \right]^{1/3} \quad (10)$$

where  $D_{F_l} d$  is based on  $\phi_l$ .

In these experiments, typical values for the Brownian diffusion coefficient of ferricyanide and the electrode diameter are  $D_B = 7.3 \times 10^{-6} \text{ cm}^2/\text{sec}$

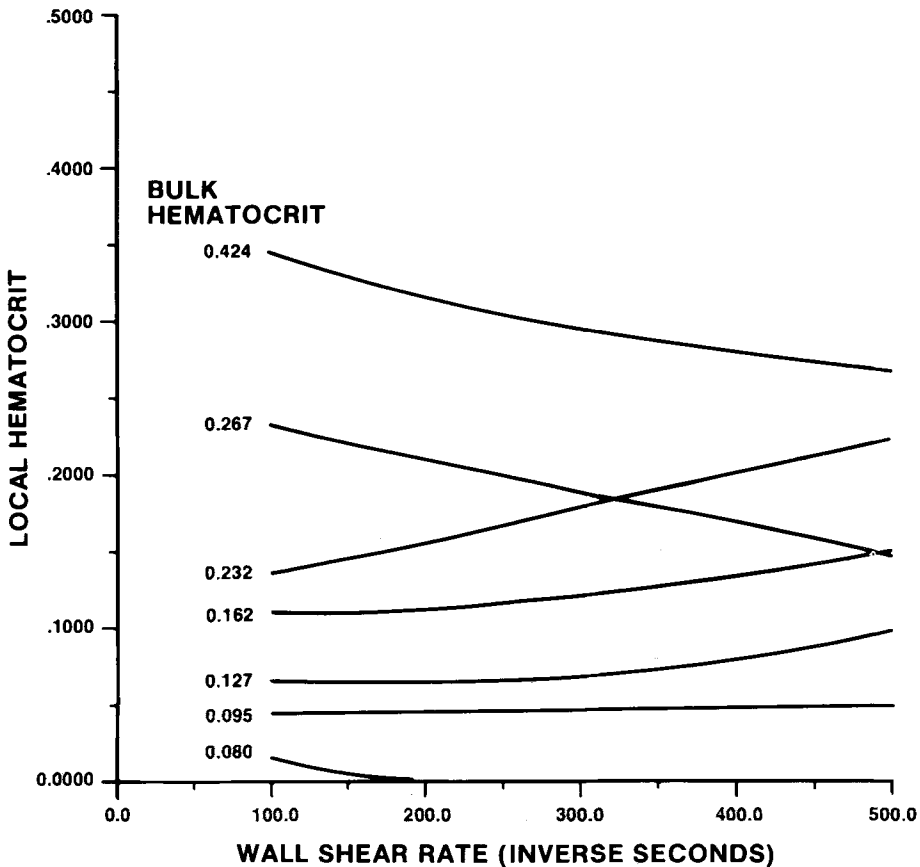


FIGURE 3. Local hematocrit vs wall shear rate.

and  $d=0.025$  cm. Using these values,  $\delta_s$  is shown as a function of wall shear rate and bulk hematocrit in Figs. 4 and 5. These curves really give a lower bound on the skimming layer thickness, since if Eq. 9 is expanded,

$$\phi_l = \frac{1}{\delta_c} \int_0^{\delta_s} \phi(y) dy + \frac{1}{\delta_c} \int_{\delta_s}^{\delta_c} \phi_b dy \quad (11)$$

For the case considered here the first integral is zero. Any other cell distribution function,  $\phi(y)$ , which is positive over the interval  $(0, \delta_s)$  will make the first integral positive. Since the sum of the two integrals is a constant, the second integral will be smaller which requires a larger  $\delta_s$  than in the case of the cell-free skimming layer.

Figures 4 and 5 indicate that different phenomena are important at various cell concentrations. At low concentrations ( $\phi_b = 0.045$ ) there are no cell interactions, the cell distribution is random and there is no skimming layer (or else the skimming layer occupies the entire tube). Increasing  $\phi_b$  to between 0.080 and 0.232 results in crowding and restriction of ro-

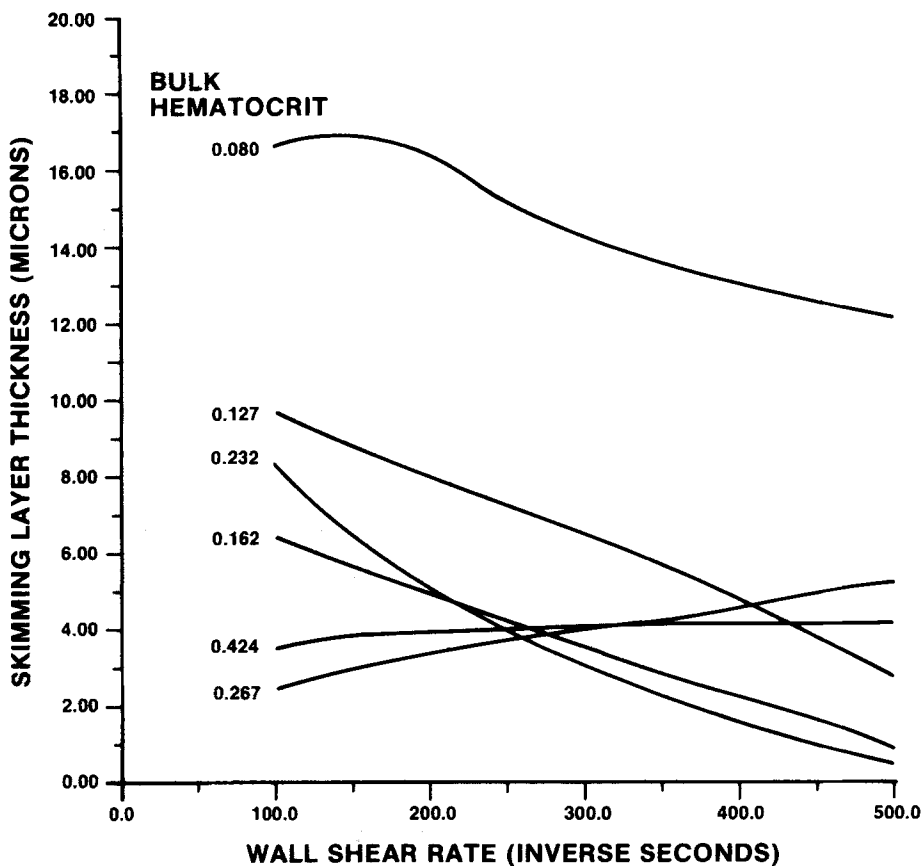


FIGURE 4. Skimming layer thickness vs wall shear rate.



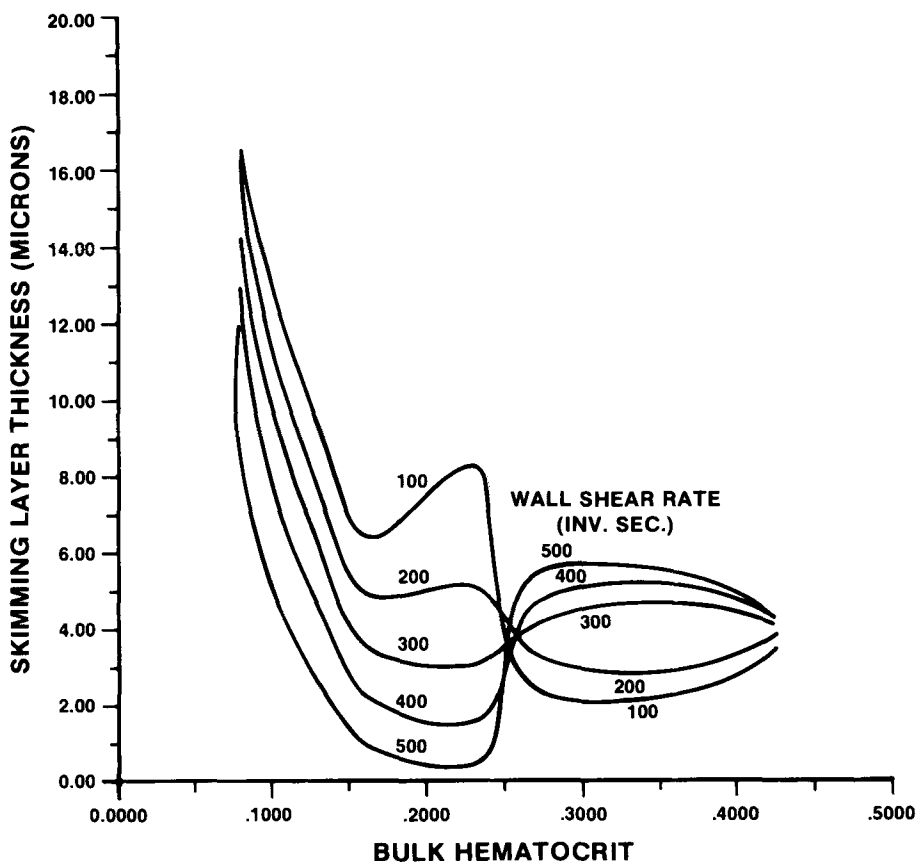


FIGURE 5. Skimming layer thickness vs bulk hematocrit.

tational freedom causing the formation of a skimming layer which becomes thinner as  $\phi_b$  increases. At about  $\phi_b = 0.25$  the deformability of the cells becomes important and the skimming layer thickness changes abruptly. The importance of cell deformability is shown clearly by Wang's results (11,12). With normal bovine cells her work shows a maximum augmentation at about  $\phi_b = 0.29$ . However, her experiments with glutaraldehyde hardened cells showed no such maximum, augmentation being an increasing monotonic function of  $\phi_b$ , while her results with ghost cells showed an order of magnitude decrease in augmentation at cell volume fractions near  $\phi_b = 0.45$  as compared with  $\phi_b = 0.09$ .

Goldsmith and Marlow (4) have observed changes in rotational modes of normal red cells as hematocrit increases. They note that for  $\phi < 20\%$  the cells were able to rotate but at higher concentrations rotation became erratic until at about  $\phi = 30\%$  the cell membrane appeared to rotate about the cell interior. They also note that hardened cells were able to rotate, even at high hematocrits. These changes in rotation modes are seen in the nonlinearity of Wang's results as expressed by the second order term in

Eq. 7. This is also reflected in Figs. 3 and 4 where the slopes of the curves change sign for  $\phi > 0.25$ .

The skimming layer thicknesses shown in Figs. 4 and 5 agree well with the observations of Bugliarello and Sevilla (1) who used an optical technique to measure the peripheral plasma layer (skimming layer) near the walls of glass tubes with diameters of 40 and 70  $\mu$ . Their results, which are for wall shear rates ranging from 570 to 3100  $\text{sec}^{-1}$ , show skimming layer thicknesses of 13  $\mu$  at a hematocrit of 0.05, decreasing to 3  $\mu$  at a hematocrit of 0.40.

The skimming layer represents a region of mass transfer resistance near the wall of a tube. Transfer through this region is controlled by both local shear rates and local hematocrits. For small molecules (such as  $\text{O}_2$ ) with relatively large values of  $D_B$  the effect of hematocrit may not be large but for large macromolecules augmentation can be significant. It is interesting to note that arguments concerning whether atherosclerotic plaques develop in high or low shear regions (5,7) ignore variations in local hematocrits that can influence augmented transport to and from the arterial wall.

## REFERENCES

1. Bugliarello, G. and J. Sevilla. Velocity distribution and other characteristics of steady and pulsatile blood flow in fine glass tubes. *Biorheology* 7:85-107, 1970.
2. Collingham, R.E. Mass transfer in flowing suspensions. Ph.D. thesis, University of Minnesota, Minneapolis, MN, 1968.
3. Fricke, H. A mathematical treatment of the electric conductivity and capacity of disperse systems. I The electric conductivity of a suspension of homogeneous spheroids. *Phys. Rev.* 24: 575-587, 1924.
4. Goldsmith, H.L. and J.C. Marlow. Flow behavior of erythrocytes. II. Particle motions in concentrated suspensions of ghost cells. *J. Coll. Interface Sci.* 71:383-407, 1979.
5. Keller, K.H. Mass transport phenomena in biological systems. In: *Bio-materials*, edited by Starke and Agarwal. New York: Plenum Press, 1969.
6. Keller, K.H. Effect of fluid shear on mass transport in flowing blood. *Fed. Proc.* 30: 1591-1599, 1971.
7. Lutz, R.J., J. N. Cannon, K. B. Bischoff, R. L. Dedrick, R. K. Stiles, and D. L. Fry. Wall shear stress distribution in a model canine artery during steady flow. *Circ. Res.* 41:391-399, 1977.
8. Petschek, H.E. and R. F. Weiss. Hydrodynamic problems in blood coagulation. AIAA paper 70-143, AIAA 3rd Fluid and Plasma Dynamics Conference, Los Angeles, 1970.
9. Reiss, L.P. and T. J. Hanratty. Measurement of instantaneous rates of mass transfer to a small sink on a wall. *AICHE J.* 8: 245-247, 1962.
10. Schwartz, A. J. Mass transport in flowing blood. Ph.D. thesis, University of Minnesota, Minneapolis, MN, 1979.
11. Wang, N.H.L. Effects of fluid shear on the mass transport properties of erythrocyte suspensions. Ph.D. thesis, University of Minnesota, Minneapolis, MN, 1978.
12. Wang, N.H.L. and K. H. Keller. Solute transport induced by erythrocyte motions in shear flow. *Trans. Am. Soc. Artif. Intern. Organs*, 25: 14-18, 1979.

## APPENDIX I

From Reiss and Hanratty (9) it is easy to show that

$$\delta_c = 1.24 \left[ \frac{D_B d}{\beta} \right]^{1/3} . \quad (12)$$

This is correct for a rectangular electrode of length  $d$ . Correcting for the presence of cells and defining the average value of  $\delta_c$  for a circular electrode as the volume under the boundary layer divided by the electrode area, we obtain Eq. 6.

## APPENDIX II

If the hematocrit in the concentration boundary layer on the electrode is  $\phi_l$  then the local effective diffusion coefficient is calculated using Eq. 2 with  $\phi = \phi_l$

$$D_{E_l} = \left[ \frac{i_l}{W \pi F n c_b d^{5/3} \beta^{1/3} (1 - \phi_l)^{1/3}} \right]^{3/2} . \quad (13)$$

Wang's (11,12) experiments tell us that (from Eq. 7)

$$D_{E_l} = D_{F_l} \left[ 1 + (a_1 \phi_l^2 + a_2 \phi_l) \text{Pe}^m \right] , \quad (14)$$

where  $D_{F_l}$  is based on  $\phi_l$ . These two values of  $D_{E_l}$  must be equal. Solving the two equations above gives us both  $D_{E_l}$  and  $\phi_l$ .